Conference Paper, Published Version

Moulin, Frédéric Y.; Peltier, Yann; Bercovitz, Yvan; Eiff, Olivier; Beer, Alexandre; Pen, Chhorda; Boulêtreau, Stéphenie; Garabétian, Frédéric; Sellali, Mehdi; Sànchez-Pérez, José; Sauvage, Sabine; Baque, David

Experimental Study of the Interaction Bewteen a Turbulent Flow and a River Biofilm Growing on Macrorugosities

EXPERIMENTAL STUDY OF THE INTERACTION BETWEEN A TURBULENT FLOW AND A RIVER BIOFILM GROWING ON MACRORUGOSITIES

Frédéric Y. Moulin[1], Yann Peltier[1], Yvan Bercovitz[1], Olivier Eiff[1], Alexandre Beer[1], Chhorda Pen[1], Stéphanie Boulêtreau[2], Frédéric Garabétian[3], Mehdi Sellali[2], José Sànchez-Pérez[2], Sabine Sauvage[2] and David Baque[2]

[1] Institut de Mécanique des Fluides de Toulouse (IMFT), UMR 5502 CNRS-INP–ENSEEIHT-UPS, Allée du professeur Camille Soula, 31400 Toulouse, France, e-mail : moulin@imft.fr

[2] Laboratoire d'Ecologie Fonctionnelle (ECOLAB), UMR 5245 CNRS-UPS-INPT, Avenue de l'Agrobiopôle, BP32607, Auzeville-Tolosane, 31326 Castanet-Tolosan, France

[3] UMR 5805 EPOC – OASU, Station Marine d'Arcachon, Université Bordeaux 1, 2 Rue du Professeur Jolyet, 33120 Arcachon cedex, France

ABSTRACT

Experiments of river biofilm growth in controlled hydrodynamic conditions were performed for a bed of large macrorugosities (4 cm diameter artificial cobbles) representative of *in situ* conditions. Local hydrodynamical conditions were measured by LDV and PIV in two successive campaigns and correlations between the turbulent boundary layer parameters and the biofilm evolution are investigated. Different biofilm structures were successfully grown for different flow conditions but their impact on local flow parameters could be clarified only for very long filaments exceeding the size of the macrorugosities. Sloughing tests were performed for 40 days old biofilms and yield results which support the hypothesis that river biofilms do not resist an increase of friction velocity beyond what they experienced during their growth.

Keywords: river biofilm, turbulent boundary layer, sloughing, flow-biofilm interaction

1. INTRODUCTION

In fluvial ecosystems dominated by fixed biomass at the bottom, the epilithic biofilm, a microbial community mainly composed of algae that grow attached to substrata, should be considered in numerical modelling of biogeochemical fluxes. Although it is a phototrophic community that requires light, the flow and the nutrient concentrations are in general the two major factors that control its accrual (see Saravia et al., 1998, Bouletreau et al. 2008). Indeed, the flow is involved directly or indirectly in many relevant processes (colonization, nutrients fluxes, sloughing) that may explain its final impact on the biofilm growth. Godillot et al (2003) found a bell curve for the biomass accumulation versus the Reynolds number for biofilm growing on gravel beds suggesting that, as for many other ecological factors, there is an optimal flow for the epilithic biofilm developpement.

Recent studies focused on a description of the flow near the bed that proved to be more pertinent that vertically integrated flow descriptors. The turbulent boundary layer near the biofilm can then be described by a friction velocity u*, a roughness length z_0 and a displacement height d, so that vertical profiles of the mean longitudinal velocity $\underline{u}(z)$ satisfy the classical log-law

$$\frac{\underline{u}}{u*} = \frac{1}{\kappa} \ln\left(\frac{z-d}{z_0}\right) \tag{1}$$

where κ is the Karman constant (κ=0.41), and the standard Reynolds decomposition is used to

define mean quantities (noted with an underline, like $\underline{u}$) and fluctuations (noted with a prime symbol, like u', defined as $u'=u-\underline{u}$).

The log-law is generally satisfied in the so called "inertial sublayer", a region confined to the lower part of the boundary layer, generally defined as $z<0.1\delta$ or $z<0.2\delta$ in most studies, with δ the boundary layer thickness (equal to the water depth D for free surface flows). Alternatively, the height of roughness of equivalent sand grain established by Nikuradse, noted k_s, can be used instead of z_0 (they are related by $k_s=30\ z_0$).

The friction velocity u* measures the drag exerted by the bottom on the flow, and retroactively, is then related to the drag exerted on the biofilm by the flow (at least when the bed is completely and homogeneously covered with a mat of biofilm). During its growth, the biofilm modifies the bottom boundary condition for the turbulent flow and different values of the roughness length z_0 are found at different stages (see Labiod et al., 2007; Godillot et al., 2003). Contradictory evolutions of z_0 were found by previous authors for biofilms growing on gravels or small size artificial substrates (see Biggs and Hickey, 1994 and Nikora et al., 1998), that enlighted the importance of the displacement height d to obtain accurate measurements of z_0. These studies also underlined the complexity of biofilm-flow interactions, with biofilm structures (length of filaments, porosity) adapting to local flow conditions.

Indeed, a description of the biofilm evolution through its sole biomass, even by including a local description of the flow (as done successfully by Labiod et al. (2007) by improving the model of Uehlinger, 1996), is not always appropriate: for instance, the autogenic sloughing triggered by high temperatures requires a separate description of the bacterial biomass (see Boulêtreau et al. 2006) ; the biofilm structure may also depend on flow conditions and yields different values of z_0 even for the same quantity of biomass ; moreover, the horizontally averaged parameters u*, z_0 and d do not represent necessarily the local hydrodynamical conditions felt by the biofilm during its growth on natural macrorugositie.

Most of the previous studies concerned growth of biofilms on small substrates (gravels or small spheres), and only a few works focused on experiments with larger substrates representative of river beds covered with cobbles (see Nikora et al., 2002). Therefore, we decided to investigate the growth of epilithic biofilm on macrorugosities and adopted the recent methodology described in Nikora et al. (2007) to calculate doubly-averaged quantities, that are shown to be more appropriate to describe turbulent canopy-like flows with strong three-dimensional patterns (see i.e. Cheng and Castro, 2002). In this paper, first results of an experimental study conducted in a specially designed indoor hydraulic flume covered with large artificial cobbles (hemispheres) are presented and discussed.

2. EXPERIMENTAL DESIGN AND MEASUREMENTS

Experiments of epilithic biofilm - turbulent flow interactions were performed in an 11-m long by 50-cm wide by 20-cm deep laboratory flume, situated on the right bank of the River Garonne at Toulouse, France. The experimental flume from Godillot et al. (2003) was adapted for the present study to be run using a partially re-circulating system opened in the River Garonne in order to benefit from natural water with no limiting nutrients and natural physico-chemical changes while controlling the hydrodynamical conditions. The flume was supplied with filtered water from the Garonne River with a flow discharge allowing a complete turnover of water in the system every 4 h. Illumination was supplied by six 1.5 m long racks of 5 neon tubes connected to a timer that ensured a photoperiod of 16 hours of day and 8 hours of night in a first campaign, and 12 hours of day and 12 hours of night in a second campaign. The bottom of the flume was completely covered by artificial cobbles, consisting in 37 mm-diameter and 20 mm in height sand-ballasted polyurethane resin hemispheres (see Figure 1). They were regularly and periodically placed on the bottom without any fixation in

order to be sampled. At the beginning of experiments, biofilms taken from a natural river and grown on artificial substrates in a laboratory were used to seed the flume (see Boulêtreau et al., 2008).

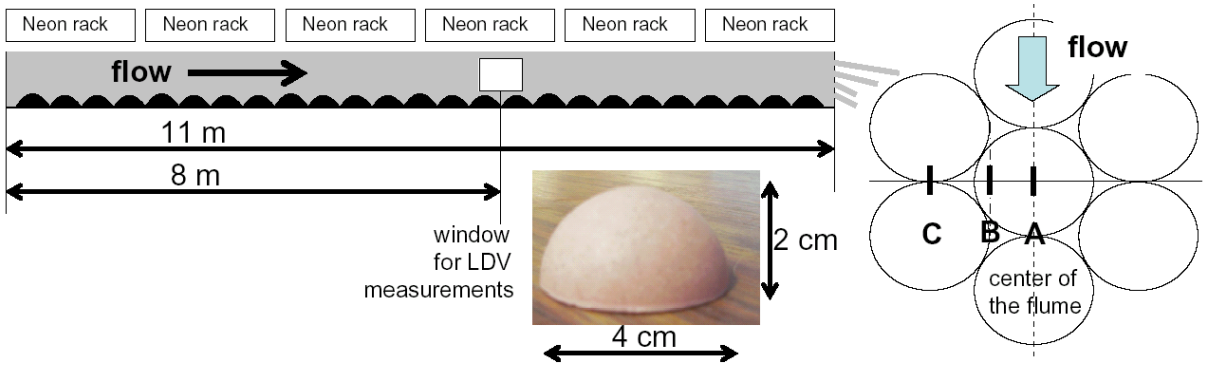

Figure 1 sketch of the laboratory flume in the first campaign, along with the dimensions of the artificial cobbles and the positions of the vertical profiles A, B and C for LDV measurements.

First campaign ; uniform flow conditions

In a first campaign, stable and uniform hydrodynamical conditions were maintained during 4 months. The biological and chemical parameters were monitored by regular samplings of the biofilm and water every week (see Boulêtreau et al., 2008). The Garonne River water was filtered at 10 µm. Velocity measurements were performed along three parallel vertical profiles (see Figure 1) at 8 m from the flume entrance by a two-components Laser Doppler Velocimeter (LDV). A discharge of 14.5 L s^{-1} in the flume and a water depth of 13.5 cm (controlled by a valve) were chosen to obtain a mean velocity of 0.22 m s^{-1} that corresponded to the optimal value of Reynolds number found by Godillot et al. (2003) for biofilm accrual on gravels.

Second campaign ; contrasted flow conditions

In a second campaign, three different flow conditions in the flume were created by modifying the width and the depth of the flume (see Figure 2), in order to obtain mean velocities of 10, 25 and 45 cm s^{-1} (respectively, in sections noted LV for low velocity, IV for intermediate velocity and HV for high velocity).

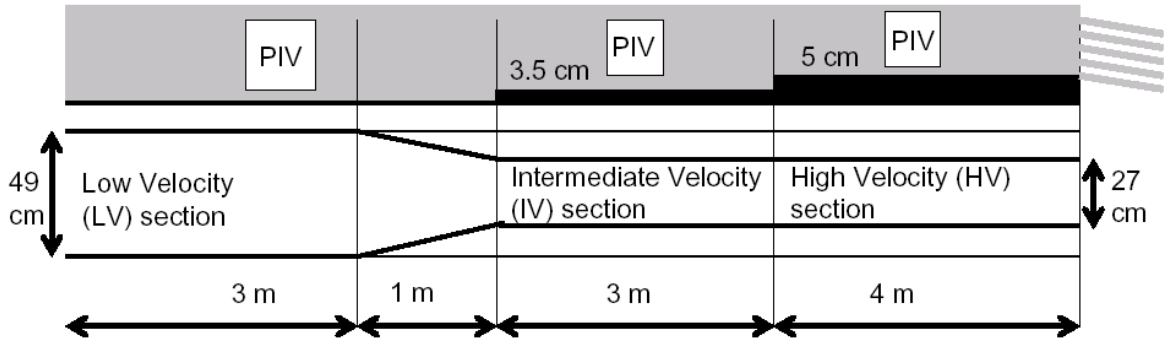

Figure 2 sketch of the modified laboratory flume in the second campaign, with locations of the PIV measurement access windows.

The Garonne River water was filtered at 1 µm in order to prevent the turbidity peaks

observed in the first campaign during floods (see Bouletreau et al., 2008). The dry mass (DM) and the ash-free dry mass (AFDM) biomasses were measured by collecting biofilm covered artificial cobbles. Biological parameters were monitored by regular samplings and photographies of the biofilm. Particle Image Velocimetry (PIV) measurements were performed in two vertical planes in the middle of the tank (one longitudinally aligned plane just over summits of hemispheres, and another one 1 cm apart) in the three different sections. The laser sheet was created by a pulsed Nd:YAG laser system (532 nm, 2×30 mJ/pulse), and the images were captured by a Sensicam camera (1280×1024 pixels, 12 bits) with resolutions from 75 to 150 pixels/cm. PIV particles were injected upstream the measurement region to improve the quality of PIV calculations (higher correlation levels).

Sloughing tests

After 40 days of growth in the three different flow regions in the second campaign, the resistance to sloughing of the three different cultivated biofilms was investigated by exposing samples to increasing flow velocities in a separate flume: a 20-m long by 21-cm wide by 40-cm deep laboratory flume whose last 12 meters were covered with artificial cobbles. A 10 cm space was left free to place the substrates covered with the 40 days old biofilm, 6 m downstream the beginning of the section covered with artificial cobbles. PIV measurements were performed for increasing discharges (5 to 30 Ls^{-1}) with a water depth maintained at 22.5 cm in the sample section by an end-valve (friction velocity u* up to 6.36 cms^{-1}). During sloughing tests, samples were exposed to discharges increasing from 5 to 30 Ls^{-1} by 5 Ls^{-1} steps every 2 minutes and monitored by a DV camera. Biomasses (DM and AFDM) were measured before (2 samples) and after (2 samples) this sloughing test for biofilms grown in the three sections.

3. RESULTS

As shown by Nikora et al. (2007), doubly-averaged quantities, i.e. quantities averaged in the two horizontal directions (noted with brackets $< >_{xy}$) must be used to describe intrinsically three-dimensional flows just over (in the so-called "roughness sublayer") and between artificial or natural macrorugosities. Such doubly-averaged quantities extend the validity range of the log-law equation (1) towards the top of the rugosities, deep inside the roughness sublayer (see Nikora et al., 2007; Cheng and Castro, 2002), yielding more robust estimations of the boundary layer parameters u*, z_0 and d.

To evaluate such quantities with LDV measurements, averaging of the three vertical profiles A, B and C was performed with weighting factors of 1, 2 and 1, respectively. With PIV measurements, averaging along the longitudinal direction x was performed for integer multiples of the spatial period of the roughness pattern (taken as the diameter of the hemispheres, 4 cm), and averaging in the y direction will be performed in the future by using the two measurement planes. In the present paper, only x-averaged quantities could be calculated from PIV measurements, but yield enough spatially converged quantities.

Turbulent boundary layer over artificial cobbles without biofilm

PIV for beds covered with artificial cobbles without biofilm were performed in the second campaign with the laboratory flume as well as during the sloughing test flume calibration. To fit the data with the log-law equation (1), we followed Cheng and Castro (2002) to determine the friction velocity u* from vertical profiles of the turbulent shear stress $<\underline{u'w'}>_x$: we took the square root of the averaged value of the turbulent shear stress in both

the roughness and inertial sublayers, i.e. in the region between the top of the hemispheres at z=H and the top of the inertial sublayer, taken as z=0.1(D-H) where D is the water depth. Typical vertical profiles of x-averaged longitudinal velocity and Reynolds stress are plotted in Figure 3. Values of the boundary layer parameters inferred from these profiles for the different experiments with artificial cobbles without biofilm are summarized in Table 1.

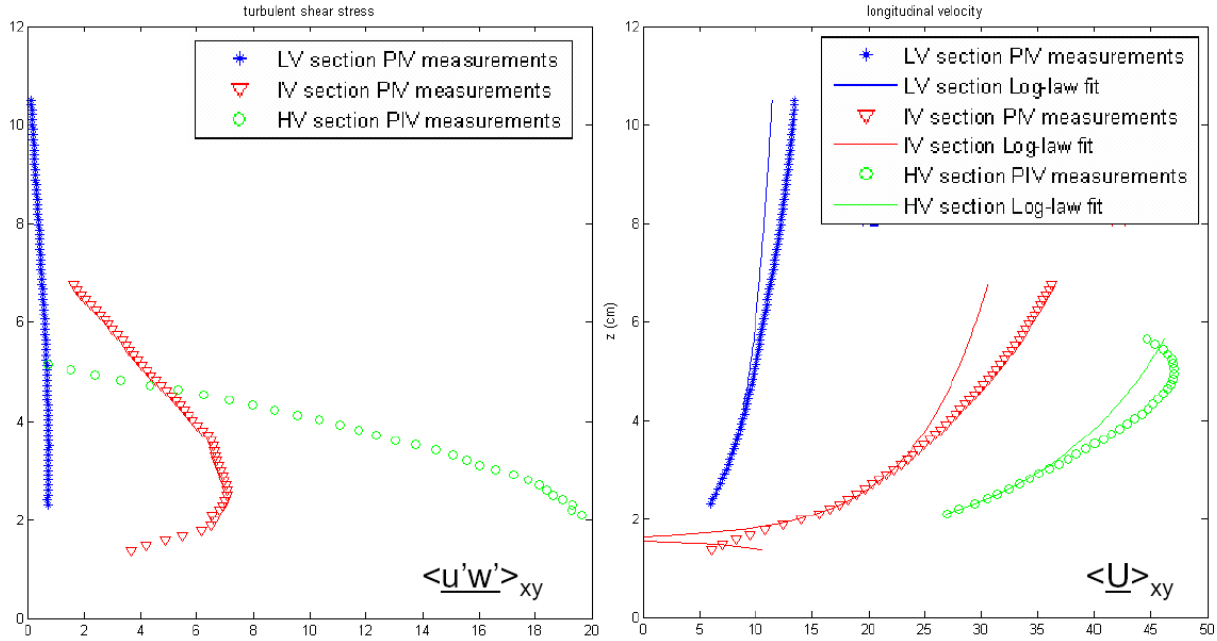

Figure 3 vertical profiles of x-averaged turbulent shear stress $\langle \underline{u'w'} \rangle_x$ and longitudinal velocity $\langle \underline{u} \rangle_x$ measured by PIV before *inoculum* in the second campaign.

Table 1 Boundary layer parameters for artificial cobbles without biofilm.

Flume Type		water depth D (cm)	flow discharge Q (Ls^{-1})	friction velocity u* (cms^{-1})	roughness length z_0 (cm)	Nikuradse grain k_s (cm)	displacement height d (cm)
Exp 2	LV	12.35	6.0	0.85	0.0396	1.19	1.61
	IV	8.35	6.0	2.61	0.0491	1.47	1.52
	HV	5.5	6.0	4.49	0.0614	1.84	1.41
Sloughing test flume		22.0	10.0	1.81	0.0323	0.97	1.56
		22.0	20.0	4.08	0.0321	0.96	1.53
		22.0	25.0	5.11	0.0348	1.05	1.55
		22.0	30.0	6.36	0.0377	1.13	1.52

Biofilm and turbulent boundary layer evolution in the first campaign

In the first campaign, a very regular and homogenous colonization pattern could be observed on the artificial cobbles (see Figure 4): initial patches located at the two front stagnation points of the flow followed by a line between them, before the biofilm spread over the whole hemisphere. Then, the biomass (DM) exhibited an exponential growth to reach a peak at 104 gm^{-2} 60 days after the *inoculum*, followed by a slow decrease towards 90 gm^{-2} during the next three weeks (see Bouletreau et al., 2008). This pattern was perturbed by a significant decrease in biomass (77% loss) due to a peak of turbidity that led to silt deposition and degradation of the first biofilm pattern. After this event, a new pattern of biofilm emerged,

with long filaments up to 15 cm undulating within the flow. Views of the biofilm at different stages along this evolution are given in figure 4.

During the LDV measurements, some difficulties were encountered with the algal filaments that moved and perturbed the acquisition. However, a top for the biofilm mat roughness could still be defined as the lowest altitude of validated measurements, and was therefore used as the lower limit for the fitting of data with the log-law profile (1). Like for measurements over nude artificial cobbles, we adopted the approach of Cheng and Castro (2002) to infer the friction velocity u* from turbulent shear stress $\langle \underline{u'w'} \rangle_{xy}$ profiles (see above) and fitted the doubly-averaged velocity profiles $\langle \underline{u} \rangle_{xy}$ to determine z_0 and d. Values of the boundary layer parameters inferred from LDV measurements during biofilm growth are given in Table 2.

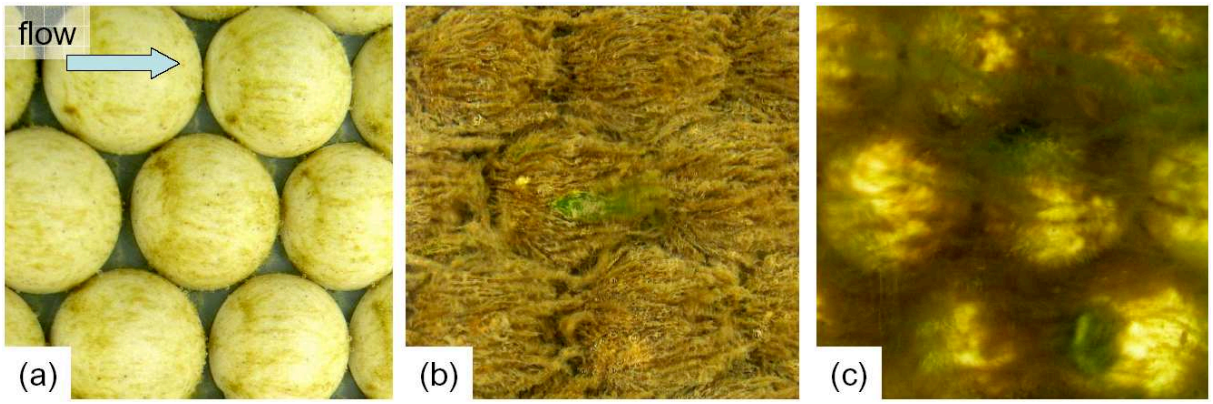

Figure 4 Biofilm patterns during the first campaign. (a) colonization phase (7 days). (b) near the end of the exponential growth phase (30 d). (c) after the turbidity peak and emergence of a new biofilm with long filaments (85 d)

Table 2 Boundary layer parameters during biofilm growth in the first campaign.

Time after *inoculum* (days d)	water depth D (cm)	DM Biomass gm^{-2}	friction velocity u* (cms^{-1})	roughness length z_0 (cm)	equivalent grain size k_s (cm)	displacement height d (cm)
30	12.80	78	2.42	0.0300	0.899	2.01
60	12.95	100	2.29	0.0204	0.611	2.94
85	12.90	24	2.15	0.0112	0.335	2.37

Biofilm and turbulent boundary layer evolutions in the second campaign

In the second campaign, regular colonization patterns were only observed in the LV section. The colonization patterns were patchy and more randomly distributed in the IV and HV sections, even if preferential locations could still be identified (see Figure 5(a) and 5(e)). Then, the biomass (DM) exhibited an exponential growth, with the formation of bubbles due to photosynthetic activity, quite numerous in the LV section (see Figure 5(b)). Eventually, a stabilisation of the biomass was observed in the three sections from the 35^{th} day after *inoculum*, with DM values around 100 gm^{-2} like in the first campaign. Yet, the biofilms in the three sections exhibited quite different structures at this stage: a thick mat in the LV section, with long and very thick filaments extending over at least two spatial wavelengths (i.e., up to 10 cm, see Figure 5(d)); more compact biofilms in the IV and HV sections (around 3 cm long and thick filaments in IV section and 3 cm long but very thin in LV).

The doubly-averaging method proved to be more difficult for these PIV measurements

than for nude artificial cobbles, algal filaments moving in the camera field. Therefore, a top for the rugosities could not be clearly identified like for solid rugosities. We used the maximal height reached by the filaments, noted z_{top}, as the lower limit of the fitting range of the log-law equation (1). Naturally, with biofilm accrual, this lower limit gradually raised up from 2 cm for the nude cobbles to 3.5 cm for the 28 days old biofilm in the low velocity section (in figure 5(d)). The upper limit of the fitting range was chosen equal to the top of the inertial sublayer at $z=z_{top}+0.2(D-z_{top})$.

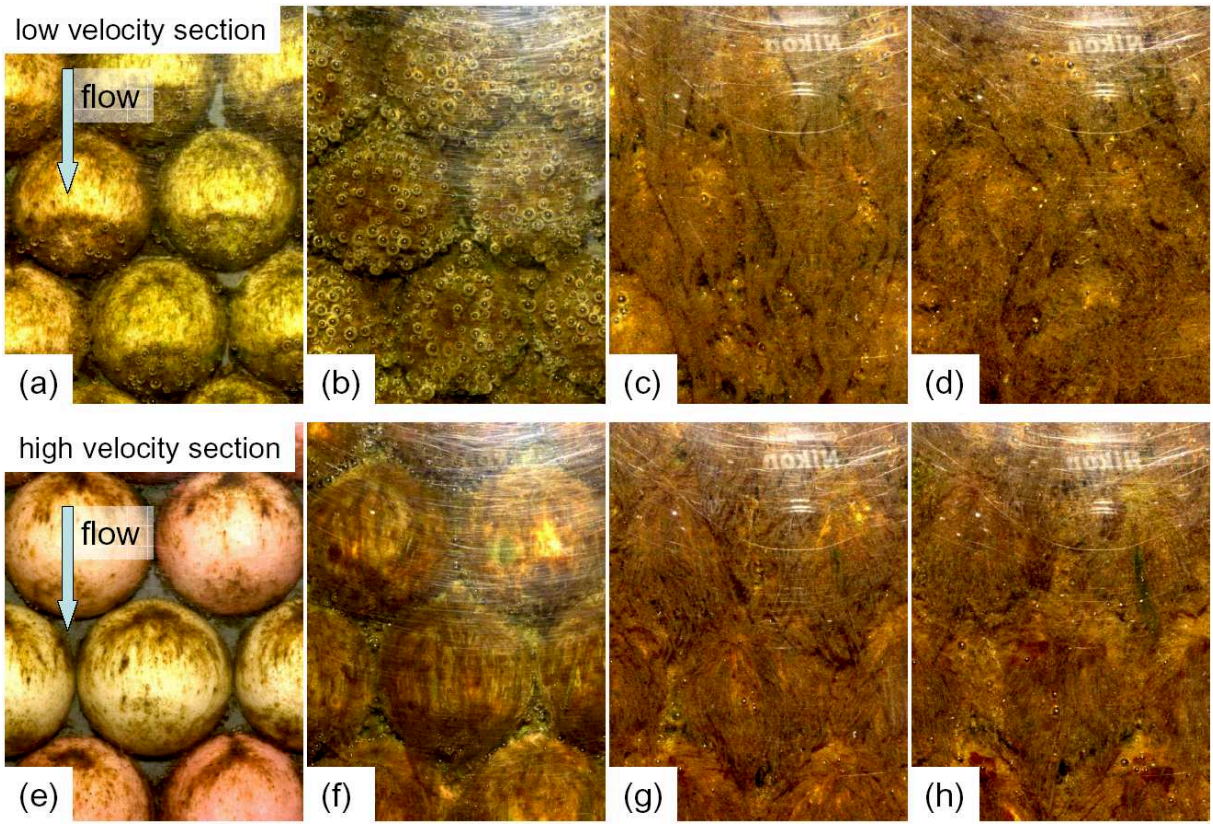

Figure 5 Top views of the epilithic biofilm evolution in the LV and HV sections at (a,e) 8, (b,f) 14, (c,g) 21 and (d,h) 28 days after *innoculum* (flow from top).

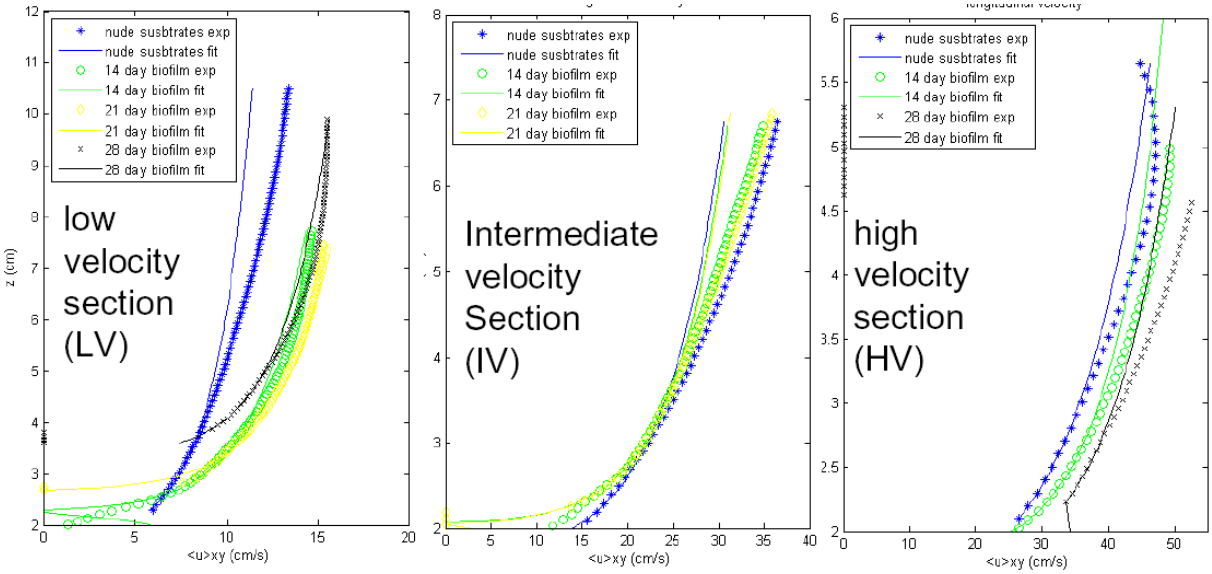

Figure 7 Evolution of x-averaged velocity profiles $\langle \underline{u} \rangle_x$ in the three sections.

Table 3 Boundary layer parameters during biofilm growth in the second campaign

Section	Age (days)	DM (gm^{-2})	D (cm)	z_{top} (cm)	u* (cms^{-1})	z_0 (cm)	k_s (cm)	d (cm)
LV	14	35	12.2	2.5	1.13	0.0349	1.05	2.19
	21	66	12.8	3.0	1.23	0.0349	1.05	2.41
	28	96	12.8	3.5	1.01	0.0121	0.36	2.86
IV	14	30	8.4	2.5	2.29	0.0196	0.589	2.02
	21	63	8.8	2.6	2.40	0.0245	0.735	2.05
HV	14	19	5.5	2.1	3.32	0.0115	0.344	1.72
	28	56	6.0	2.5	3.63	0.0106	0.318	1.84

Resistance to sloughing of biofilms grown in different conditions

After 40 days in the second campaign, four large samples (composed of at least of 12 artificial cobbles fixed on a PVC plate) were collected in each section and two of them were exposed to increasing flow conditions in the sloughing test flume (u* up to 6.36 cms^{-1}, see Table 1). Biomass measurements for samples without and with sloughing test are given in table 4. Sloughing occurs almost as soon as the friction velocity value exceeds the time-averaged value in the considered growth section. A part of the biofilm strongly attached to the artificial cobbles always remains after this sloughing test (biomass measured after sloughing test in Table 4), while a part composed mostly of filaments was taken away by the flow.

Table 4 Measurements of biomass (DM) for a sloughing test up to u*=6.36 cms^{-1}

Flume section	u* during growth (averaged, cms^{-1})	DM biomass without sloughing (gm^{-2})	DM biomass after sloughing (gm^{-2})	Detached proportion
LV	1.0	121.4	57.9	52%
IV	2.5	100	70.7	29%
HV	4.0	104.5	93.5	11%

5. DISCUSSION

The turbulent boundary layer parameters obtained for the artificial cobbles without biofilm (see Table 1) are in good agreement with previous works on artificial canopy flows: values of d are close to 0.75H that is widely used to estimate d for log-law profiles over canopies ; values of k_s are all around 1 cm for large aspect ratio flows (i.e. with D=12 cm) meaning that the hemispheres of radius 2 cm generate a boundary layer similar to a bed of 1 cm radius sand. As the confinement increases (D/H=4 and 3 in the IV and HV sections at the beginning of the experiment), larger values of k_s and smaller values of d are measured, in agreement with the trend observed by Bayazit (1976) for steep shallow flows over hemispheres.

For biofilm growing on artificial cobbles in relatively deep water conditions (D≈12 cm), no significant modification of the roughness length was observed as long as the biofilm structure remains relatively compact. This was the case in the first growth sequence of the first campaign with a moderate value of the friction velocity (see Table 2), as well as in the first phase of growth in the LV section for the second campaign (see Table 3). In both cases, k_s values remain initially close to the value found for artificial cobbles without biofilm, i.e. 1 cm. In our experiments, no increase of k_s was observed for biomass values and biofilm

structures that present visual similarities with the biofilm grown in Nikora et al. (2002), who measured a 20% increase for this parameter. However, a very clear drop in k_s (towards values close to 0.35 cm) was measured as soon as long and thick filaments became dominant. In the first campaign it was triggered by a turbidity peak that changed the biofilm species composition (see Boulêtreau et al. 2008). In the second campaign, low friction velocity conditions allowed the growth of a thick but porous mat of long and thick filaments that exceeded the initial spatial wavelength prescribed by the artificial cobbles (see Figure 5(d)).

In contrast, for biofilm growing on macrorugosities in shallow water conditions (i.e. when the vertical dimension of the roughness is not small in comparison with water depth), the evolution is very different. In the IV and HV sections in the second experiment, very confined flows are generated initially (D/H=4 and 3), and a very quick drop in k_s is observed (see Table 3). One major difficulty here is the very strong dependence of this parameter with the chosen fitting range for the log-law profile: the available interval is small since it scales as 0.1(D-H) (respectively around 0.65 and 0.4 cm for IV and HV sections) and the lower position is not easily defined for algal rugosities. Indeed, the structure of the boundary layer for very confined flows is actually questioned and it is not clear if and where a log-law should apply when D/H becomes large. Therefore, the large drop in k_s measured in IV and HV sections when cobbles are covered by a filamentous biofilm could be also associated with a drop of the confinement effect that should be a function of k_s/D or $(z_0-d)/D$, rather than H/D (that can be defined precisely only for hemispheres without biofilm).

Consistent with Paterson (1996), biofilms with different structures were nevertheless successfully triggered by different flow conditions in the second campaign, and clear different resistances to sloughing could be assessed by exposing samples to increasing flow velocities.

6. CONCLUSION

Laboratory experiments of river biofilm growth on artificial cobbles representative of what occurs *in situ* were successfully conducted, and allowed precise measurements of the bottom flow conditions. In contrast with previous studies where the biofilm was grown on small substrates that were quickly covered (see Godillot and al., 2003; Labiod and al., 2007), fully turbulent flows (with $k_s^+=k_s u^*/\nu>30$) were generated here, and the biofilm was not necessarily covering completely the artificial substrates. As a consequence, competitive contributions from the wake and skin frictions behind cobbles and along algal filaments seem to drive a complex evolution of the roughness length since this quantity integrates all the processes occurring in the canopy (see Nikora et al., 2007a,b). A drop of k_s in deep flows is nevertheless shown to be associated with filaments longer than the initial horizontal scale prescribed by the substrates, a pattern that occurs in low velocity flows for usual river biofilms. It should be pointed that the range of observed z_0 values (0.3 to 1.8 cm) is far narrower than the one obtained for biofilm growth on smaller substrates (see Godillot et al 2003; Labiod et al., 2007), another consequence of the mixed contributions from the biofilm structure and the substrates on which it grows.

The impact of different flow conditions on the biofilm structure could be clearly put in evidence by camera recordings. On the one hand, this structural difference that influences the biofilm retroaction on the flow and its resistance to hydrodynamical changes is surprisingly very poorly correlated with the biomass indicators (DM and AFDM) used in the experiments. On the other hand, both the structure and the resistance of the biofilm to increased flow velocities seem to be function of the friction velocity u* of the boundary layer where it was grown. In this context, the results of sloughing tests give a new light on the role of the catastrophic detachment term associated with floods in the predictive equation of Uehlinger (1996) for biofilm biomass. The improvement of Labiod and al. (2007) for the chronic

detachment term of Uehlinger (1996) has still to be extended to biofilms on large macrorugosities, where the relation between the friction velocity u* and the exchanges of matter from the canopy to the free stream is still a non-resolved issue (see Moulin et al., 2007).

REFERENCES

Bayazit M. (1976). Free surface flow in a channel of large relative roughness. *Journal of Hydraulic Research*, 14 : 115–126.

Biggs, B.J.F. and Hickey C.W. (1994). Periphyton responses to a hydraulic gradient in a regulated river in New Zealand. *Freshwater Biology*, 32 : 49-59.

Boulêtreau S., Garabetian F., Sauvage S. and Sánchez-Pérez J.M. (2006). Assessing the importance of self-generated detachement process in river biofilm models. *Freshwater Biology*, 51 : 901-912.

Boulêtreau S, Sellali M., Bercovitz Y., Nicaise Y., Sauvage S., Sánchez-Pérez J-M., Moulin F.Y., Eiff O. and Garabétian F. (2008), Long-term dynamics of epilithic biomass in controlled flows: structural and functional changes. *Submitted to Aquatic Sciences*.

Cheng H. and Castro I.P. (2002), Near wall flow over urban-like roughness. *Bound. Layer Meteorol.*, 104, 229-259.

Godillot R., Ameziane T., Caussade B. and Capblanc J. (2003), Interplay between turbulence and periphyton in rough open-channel flow. *Journal of Hydraulic Research*, 39(3): 227-239.

Labiod C., Godillot R. and Caussade B. (2007), The relationship between stream periphyton dynamics and near-bed turbulence in rough open-channel flow. *Ecological Modelling*, 209: 78-96.

Moulin F. Y., Guizien K., Thouzeau G., Chapalain G., Mülleners K. and Bourg C. (2007), Impact of an invasive species, Crepidula fornicata, on the hydrodynamics and transport properties of the benthic boundary layer. *Aquatic Living Resources*, 20: 15-31.

Nikora V.I., Goring D.G. & Biggs B.J.F. (1998), A simple model of stream periphyton – flow interactions. *Oikos*, 81 : 607– 611.

Nikora V.I., Goring D.G. and Biggs B. J. F. (2002), Some observations of the effects of micro-organisms growing on the bed of an open channel on the turbulence properties. *Journal of Fluid Mechanics*, 450 : 317-341.

Nikora V., McEwan I., McLean S., Coleman S., Pokrajac D. and Walters R. (2007a), Double-averaging Concept for rough-Bed Open-Channel and overland flows: theorical background. *Journal of Hydraulic Engineering*, 133(8) : 873-883.

Nikora V., McLean S., Coleman S., Pokrajac D., McEwan I., Campbell L., Aberle J., Clunie D. and Koll K. (2007b), Double-averaging Concept for rough-Bed Open-Channel and overland flows: applications background. *Journal of Hydraulic Engineering*, 133(8) : 873-883.

Saravia L. A., Momo F. and Boffi Lissin L. D. (1998), Modelling periphyton dynamics in running water. *Ecological Modelling*, 114 : 35-47.

Uehlinger U., Buhrer H. and Reichert P. (1996), Periphyton dynamics in a floodprone prealpine river : evaluation of significant processes by modelling. *Freshwater Biology*, 36 : 249-263.